01

The effect of anisotropy of an isoenergetic surface on the electrical conductivity of a thin conductive film in a longitudinal magnetic field

© I.A. Kuznetsova, O.V. Savenko, D.N. Romanov

Demidov State University,
150003 Yaroslavl, Russia
e-mail: romanov.yar357@mail.ru

Received September 19, 2023
Revised March 30, 2024
Accepted April 1, 2024

An analytical expression of the electrical conductivity of a thin conductive film in a longitudinal magnetic field is obtained considering an ellipsoidal isoenergetic surface. The model of diffuse boundary conditions is used as boundary conditions for the charge carrier distribution function. The limiting cases of degenerate, non-degenerate electron gas, spherical isoenergetic surface are considered. The dependence on the effective mass is shown. A comparative analysis of theoretical calculations with experimental data is carried out.

Keywords: thin film, kinetic equation, Fuchs model, isoenergetic surface, longitudinal magnetic field.

DOI: 10.61011/TP.2024.05.58513.243-23

Introduction

Thin film technology ensures creation of thin conductive layer applied in photonics and nanophotonincs [1,2], microwave electronics [3,4], sun energy [5–9]. „Thin" films are films which thickness is comparable or below electron mean free path. As technology develops the density of semiconductor devices on integrating circuit increases. In this relation large requirements are applied to quality of parameters of conductive layers which comprise the semiconductor devices.

When film thickness becomes comparable to the mean free path of charge carriers, the contribution of surface scattering to the electrical properties of this film increases, for example, electric conductivity decreases, Hall coefficient increases etc. If the film contains quantum size effects, i.e. its thickness if much larger the de Broglie wavelength of charge carrier moving with average speed then for calculation of the film electrical parameters it is sufficient ti use the kinetic equation true in the quasi-classic approximation.

During last decade papers were published associated with theoretical and experimental studies of electrical and galvanomagnetic properties of thin conductive films. Paper [10] present a new model of electric conductivity of thin polycrystalline film. Articles [11–13] showed the experimental effect of longitudinal, transverse and perpendicular magnetic fields on the resistivity of thin films of gold with grain structure at temperatures 4–50 K and comparison with theoretical calculations based on Boltzmann kinetic equation.

Calculation of the conductivity of thin metal layer in case of different specularity coefficients of its surfaces were carried out in the papers [14,15]. High frequency conductivity in the transverse magnetic field was calculated in paper [16], and in longitudinal magnetic field — in paper [17]. To solve objectives in the above papers the standard kinetic method was used, it means solution of the kinetic equation with appropriate limit conditions. This method of solution was used also to study the electric and galvanomagnetic properties of thin metal wires. So, in paper [18] the self-inductance of the thin metal wire was determined.

The dispersion law (dependence of quasi-particle energy on pulse) has significant effect on the motion nature of electrons (holes) in semiconductor. constant energy surface of bismuth for electrons is three ellipsoids of revolution whose axes of rotation lie in the same plane, and angle between these axes is $2\pi/3$. The calculation of high frequency conductivity of thin metal layer in case of Fermi ellipsoid surface is given in article [19]. The present paper provides comparison of experimental data and theoretical calculations relating dependence of magneto resistance on induction of the external magnetic field of the bismuth film, as this material has high anisotropy of constant energy surface. As compared to other semiconductors the bismuth has advantage of easy manufacturing of high quality single-crystals with large mean free path of electron, reaching about 1 mm. this ensures better study of the classic size effect, when the film thickness becomes below the mean free path of electron or hole.

In present paper using the kinetic approach the effect of anisotropy of constant energy surface on the conductivity of thin conductive film in longitudinal magnetic field is studied. The film is nonmagnetic and single-crystal. External fields are homogeneous, skin effect and plasma resonance are not considered (frequency of external electric field is rather small).

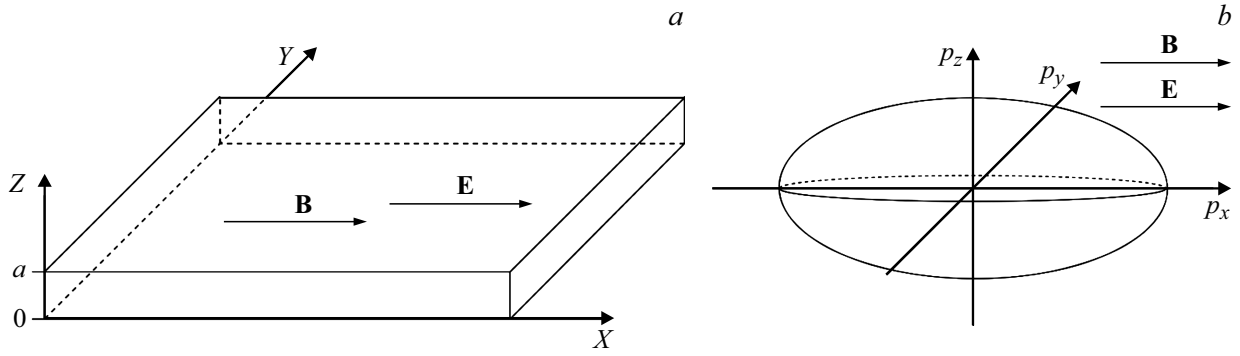

Figure 1. a — thin conductive film, b — constant energy surface of film material.

1. Problem formulation

Let's consider thin film laying in plane XOY. Conductor is film material. The conductor is metal or semiconductor with arbitrary degree of degeneration. Film thickness a is much larger the de Broglie wavelength of charge carrier moving with average speed, so we can neglect the quantum size effects. Along axis X the magnetic field with induction $\mathbf{B}$ and electric field with strength $\mathbf{E}$ are directed (Fig. 1, a). The film is in vacuum or located between two insulating layers that do not allow current passage through the film boundaries. Electric field is homogeneous and experiences harmonic oscillations with a frequency ω:

$$\mathbf{E} = \mathbf{E}_0 \exp(-i\omega t). \tag{1}$$

Let's assume that constant energy surface of the conductor has form of three-axes ellipsoid. Si, Ge, Bi and other materials have such form of surface. Let's semi-axes of ellipsoid lay along pulse axes like in Fig. 1, b. In this case the dispersion law is

$$\varepsilon = \frac{p_x^2}{2m_1} + \frac{p_y^2}{2m_2} + \frac{p_z^2}{2m_3}, \tag{2}$$

where m_1, m_2, m_3 — effective masses along axes p_x, p_y, p_z.

To determine the conductivity of film the distribution function f is used. If system deviation for equilibrium position is minor, i.e. external fields are low, the problem can be linearized

$$f(\mathbf{p}, z, t) = f_0(\varepsilon) + f_1(\mathbf{p}, z)\exp(-i\omega t), \tag{3}$$

$$f_0(\varepsilon) = [1 + \exp((\varepsilon - \mu)/k_B T)]^{-1}, \tag{4}$$

where f_0 — Fermi–Dirac equilibrium distribution function (zero approximation), and f_1 — small correction (first approximation), ensuring low external effect, μ — electrochemical potential, k_B — Boltzmann constant, T — temperature.

The distribution function obeys the kinetic equation. This equation in the relaxation time approximation τ looks like

$$-i\omega f_1 + v_z \frac{\partial f_1}{\partial z} + e(\mathbf{v}\cdot\mathbf{E}_0)\frac{\partial f_0}{\partial \varepsilon} + e[\mathbf{v}\times\mathbf{B}]\frac{\partial f_1}{\partial \mathbf{p}} = -\frac{f_1}{\tau}, \tag{5}$$

where $\mathbf{v}$ — speed vector of charge carriers.

For unambiguous determination of distribution function we use Fuchs diffuse-specular boundary conditions model [20]:

$$\begin{cases} f(v_z, 0) = q_1 f(-v_z, 0) + (1 - q_1) f_0, \\ f(-v_z, a) = q_2 f(v_z, a) + (1 - q_1) f_0, \end{cases} \tag{6}$$

where q_1 and q_2 — specularity coefficients of bottom and top surfaces.

System of equations (6) considering (3) is converted into

$$\begin{cases} f_1(v_z, 0) = q_1 f_1(-v_z, 0), \\ f_1(-v_z, a) = q_2 f_1(v_z, a). \end{cases} \tag{7}$$

Current density can be determined based on the determined distribution function $\mathbf{j}$:

$$j = en\langle\mathbf{v}\rangle = e\int \mathbf{v} f_1 \frac{2d^3p}{h^3}, \tag{8}$$

where h — Planck's constant, n — concentration of current carriers:

$$n = \int f_0 \frac{2d^3p}{h^3}. \tag{9}$$

2. Method of solution and mathematical calculations

Due to anisotropy of constant energy surface (2) the projection of trajectory of charge carriers on plane YOZ

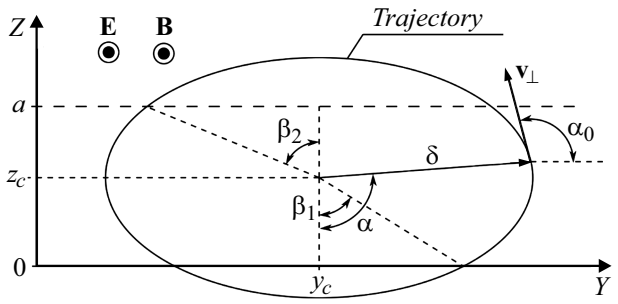

Figure 2. Trajectory of charge carriers in plane YOZ.

is ellipse (Fig. 2). The ellipse is described by the following equation:

$$\left(\frac{y-y_c}{y_{01}}\right)^2+\left(\frac{z-z_c}{z_{01}}\right)^2=1, \tag{10}$$

$$y_{01}=\frac{\sqrt{2m_2\varepsilon_\perp}}{Be}\quad, z_{01}=\frac{\sqrt{2m_2\varepsilon_\perp}}{Be}, \tag{11}$$

$$\varepsilon_\perp=\frac{p_y^2}{2m_2}+\frac{p_z^2}{2m_3}, \tag{12}$$

where y_c and z_c — coordinates of ellipse center, y_{01} and z_{01} — ellipse semi-axes.

Depending on the trajectory, the expression for the distribution function will take a different form. Trajectory of electrons (holes) cab intersect only top border of film (which corresponds to the distribution function f_1^u), only bottom border (f_1^d), top and bottom (f_1^{ud}), neither of borders (f_1^v). The kinetic equation (5) depending of the trajectory position is solved by the same method as in paper [7].

$$f_1^u(\nu t',\nu T')=-\frac{ev_xE_0}{\nu}\left(\frac{\partial f_0}{\partial\varepsilon}\right)\left[1-\frac{(1-q_2)e^{-\nu t'}}{1-q_2e^{-\nu T'}}\right], \tag{13}$$

$$f_1^d(\nu t',\nu T')=-\frac{ev_xE_0}{\nu}\left(\frac{\partial f_0}{\partial\varepsilon}\right)\left[1-\frac{(1-q_1)e^{-\nu t'}}{1-q_1e^{-\nu T'}}\right], \tag{14}$$

$$f_1^d(\nu t',\nu T')=\begin{cases}-\frac{ev_xE_0}{\nu}\left(\frac{\partial f_0}{\partial\varepsilon}\right)\left[1-\frac{1-q_1+q_1(1-q_2)e^{-\nu t'}}{1-q_1q_2e^{-2\nu T'}}e^{-\nu t'}\right] \\ \qquad \text{for}\quad \nu_z>0, \\ -\frac{ev_xE_0}{\nu}\left(\frac{\partial f_0}{\partial\varepsilon}\right)\left[1-\frac{1-q_2+q_2(1-q_1)e^{-\nu t'}}{1-q_1q_2e^{-2\nu T'}}e^{-\nu t'}\right] \\ \qquad \text{for}\quad \nu_z<0,\end{cases} \tag{15}$$

$$f_1^v=-\frac{(ev_xE_0}{\nu}\left(\frac{\partial f_0}{\partial\varepsilon}\right), \tag{16}$$

where $\nu=\tau^{-1}-i\omega$ — complex scattering frequency, t' — time of charge carrier movement from moment of last scattering on film surface to current point which position is characterized by vector $\boldsymbol{\delta}$, T' — the time of electron (hole) movement between two successive scatterings on the film surfaces.

If the scattering occurs on top surface then $a-z_c<z_{01}$, otherwise $a-z_c>z_{01}$ (Fig. 2). If scattering occurs on bottom surface then $z_c<z_{01}$, otherwise $z_c>z_{01}$. In this case, the general distribution function can be written as follows:

$$f_1=f_1^u\Theta(-A1)\Theta(A_2)+f_1^d\Theta(A_1)\Theta(-A_2)+f_1^{ud}\Theta(A_1)\Theta(A_2)+f_1^v\Theta(-A_1)\Theta(-A_2), \tag{17}$$

$$A_1=1-\frac{z_c}{z_{01}},\qquad A_2=1-\frac{a-z_c}{z_{01}}, \tag{18}$$

where $\Theta(x)$ — Heaviside function:

$$\Theta(x)=\begin{cases}0, & x<0,\\ 1, & x\geq 0.\end{cases} \tag{19}$$

Let's express t' and T' through coordinates

$$t'=\int\limits_{\alpha_1'}^{\alpha}\frac{ds}{v_\perp},\qquad T'=\int\limits_{\alpha_1'}^{\alpha_2'}\frac{ds}{v_\perp},$$

$$v_\perp=\frac{\sqrt{2\varepsilon_\perp}}{\sqrt{m_2\cos^2\alpha_0+m_3\sin^2\alpha_0}}, \tag{20}$$

$$ds=\sqrt{\delta^2+\left(\frac{\partial\delta}{\partial\alpha}\right)^2}d\alpha,$$

$$\delta=\frac{\sqrt{m_2m_3}}{Be}\frac{\sqrt{2\varepsilon_\perp}}{\sqrt{m_2\cos^2\alpha+m_3\sin^2\alpha}}, \tag{21}$$

where t' and T' — times of movement of charge carrier with positive ($\alpha_0\in[0;\pi]$) or negative ($\alpha_0\in[\pi;2\pi]$) projection of speed v_z from time when sign of this speed projection v_z changed, till current time moment or till next time when sign of speed projection v_z changes again, respectively; α — angle between vector $(0,0,-1)$ and vector $\boldsymbol{\delta}$ (shown in Fig. 2); α_0 — angle between axis Y and transverse speed $\mathbf{v}_\perp$ (shown in Fig. 2). Integration limits α_1' and α_2' depend on what film surfaces the electron (hole) is scattered and on values α_0, i.e. sign of speed projection v_z. Values of these limits are given in Table.

integration limits

Functions	$\alpha_0\in[0;\pi]$		$\alpha_0\in[\pi;2\pi]$	
f_1^d	β_1	π	π	$2\pi-\beta_1$
f_1^u	0	$\pi-\beta_2$	$\pi+\beta_2$	2π
f_1^{ud}	β_1	$\pi-\beta_2$	$\pi+\beta_2$	$2\pi-\beta_1$

Variable α_0 depends on α. The ellipse coordinates depend on angle α (Fig. 2)

$$\begin{cases} y = y_c + \delta \sin\alpha, \\ z = z_c - \delta \cos\alpha. \end{cases} \tag{22}$$

Angle α_0 is angle of tangent inclination to ellipse (Fig. 2), so

$$\operatorname{tg}\alpha_0 = \frac{dz}{dy}. \tag{23}$$

If we take derivative of the ellipse equation (10) considering (22) and (23), then we obtain the relationship between angles α_0 and α:

$$\operatorname{tg}\alpha_0 = \frac{m_2}{m_3}\operatorname{tg}\alpha. \tag{24}$$

For current density (8) calculation it is convenient to move to new variables $(p_x, p_y, p_z) \to (\varepsilon_\perp, \alpha_0, v_x)$:

$$\begin{cases} p_x = m_1 v_x, \\ p_y = \frac{m_2\sqrt{2\varepsilon_\perp}\cos\alpha_0}{\sqrt{m_2\cos^2\alpha_0 + m_3\sin^2\alpha_0}}, \\ p_z = \frac{m_3\sqrt{2\varepsilon_\perp}\sin\alpha_0}{\sqrt{m_2\cos^2\alpha_0 + m_3\sin^2\alpha_0}} \end{cases} \tag{25}$$

It is expected that scattering length on admixtures is lower than electron-electron interaction length. In this case heterogeneous hydrodynamic flow of electrons is not formed in the film. Heterogeneity of current across the channel is insufficiently strong to be detected by methods suggested for such heterogeneity detection in articles [21–23], as the film thickness is small. Let's determine average through film thickness current

$$\langle j_x \rangle = \frac{1}{a}\int_0^a j_x dz. \tag{26}$$

Specific conductivity will be determined from formula of local Ohm law:

$$\sigma_x = \langle j_x \rangle / E_0. \tag{27}$$

Let's introduce the dimensionless parameters:

$$m_0 = \sqrt[3]{m_1 m_2 m_3}, \quad k_{m1} = m_1/m_0,$$
$$k_{m2} = m_2/m_0, \quad k_{m3} = m_3/m_0, \tag{28}$$
$$n v_1^2 = \frac{5}{3}\int v^2 f_0 \frac{2d^3p}{h^3},$$
$$u_1 = \frac{m_0 v_1^2}{2k_B T} = \frac{5}{9}\left(\frac{1}{k_{m1}} + \frac{1}{k_{m2}} + \frac{1}{k_{m3}}\right)\frac{I_1}{I_0}, \tag{29}$$
$$I_j = \int_0^\infty \frac{u^j\sqrt{u}du}{1+e^{u-u_\mu}}, \quad k_{m\alpha_0} = k_{m2}\cos^2\alpha_0 + k_{m3}\sin^2\alpha_0, \tag{30}$$
$$a_0 = a/\lambda, \quad \omega_0 = \lambda\omega/v_1,$$
$$\nu_0 = a\nu/v_1 = \lambda_0(1 - i\omega_0), \tag{31}$$
$$\beta_0 = \lambda e B/(m_0 v_1), \qquad \xi = z/a, \tag{32}$$
$$u_\mu = \mu/(k_B T), \qquad u_\perp = \varepsilon_\perp/(k_B T),$$
$$u_x = m_0 v_x^2/(2k_B T), \qquad u = k_{m1}u_x + u_\perp, \tag{33}$$

where m_0 — effective mass of density of states; k_{m1}, k_{m2} and k_{m3} — dimensionless effective masses along axes p_x, p_y and p_z respectively; v_1 — characteristic speed introduced via expression (29) [21]; a_0 — dimensionless film thickness; $\lambda = v_1\tau$ — mean free path of electron (hole); ω_0 — dimensionless frequency of external electric field; β_0 — dimensionless induction of magnetic field.

Omitting mathematical transformations, we obtain expressions for specific conductivity(27):

$$\sigma(a_0, \omega_0, \beta_0, k_{m1}, k_{m2}, q_1, q_2, u_\mu) = \sigma_0 \sum(a_0, \omega_0, \beta_0, k_{m1}, k_{m2}, q_1, q_2, u_\mu), \tag{34}$$
$$\sigma_0 = (ne^2\tau)/m_0, \tag{35}$$
$$\Sigma = \frac{a_0}{2\pi\nu_0 I_0}\int_0^\infty\int_0^\infty \frac{\sqrt{u_x}e^{u-u_\mu}}{(1+e^{u-u_\mu})^2} \times (B_1 + B_2 + B_3 + B_4 + B_5)du_\perp du_x, \tag{36}$$
$$B_1 = \int_0^1\int_0^\pi 2\left[1 - \frac{(1-q_1)e^{-\nu t_1'}}{1-q_1 e^{-\nu T_1'}}\right]\frac{\Theta(A_1)\Theta(-A_1)}{k_{m\alpha_0}}d\alpha_0 d\xi, \tag{37}$$
$$B_2 = \int_0^1\int_0^\pi 2\left[1 - \frac{(1-q_2)e^{-\nu t_2'}}{1-q_2 e^{-\nu T_2'}}\right]\frac{\Theta(-A_1)\Theta(A_1)}{k_{m\alpha_0}}d\alpha_0 d\xi, \tag{38}$$
$$B_3 = \int_0^1\int_0^\pi \left[1 - \frac{1-q_1+q_1(1-q_2)e^{-\nu T_3'}}{1-q_1 q_2 e^{-2\nu T_3'}}e^{-\nu t_1'}\right] \times \frac{\Theta(A_1)\Theta(A_2)}{k_{m\alpha_0}}d\alpha_0 d\xi, \tag{39}$$
$$B_4 = \int_0^1\int_0^\pi \left[1 - \frac{1-q_2+q_2(1+q_1)e^{-\nu T_3'}}{1-q_1 q_2 e^{-2\nu T_3'}}e^{-\nu t_1'}\right] \times \frac{\Theta(A_1)\Theta(A_2)}{k_{m\alpha_0}}d\alpha_0 d\xi, \tag{40}$$
$$B_5 = \int_0^1\int_0^\pi 2\frac{\Theta(-A_1)\Theta(-A_2)}{k_{m\alpha_0}}d\alpha_0 d\xi, \tag{41}$$
$$\nu t_1' = \int_{\beta_1}^\alpha dC_t, \quad \nu t_2' = \int_0^\alpha dC_t, \tag{42}$$
$$\nu T_1' = \int_{\beta_1}^\pi dC_t, \quad \nu T_2' = \int_0^{\pi-\beta_2} dC_t, \quad \nu T_3' = \int_{\beta_1}^{\pi-\beta_2} dC_t, \tag{43}$$

$$dC_t = \frac{\nu_0\sqrt{k_{m\alpha_0}k_{m2}k_{m3}}}{a_0\beta_0}\sqrt{\tilde{\delta}^2 + \left(\frac{\partial\tilde{\delta}}{\partial\alpha}\right)^2}\,d\alpha,$$

$$\tilde{\delta} = \frac{1}{\sqrt{k_{m2}\cos^2\alpha + k_{m3}\sin^2\alpha}}, \tag{44}$$

$$\cos\beta_1 = A_1 = 1 - \sqrt{\frac{u_1}{k_{m2}u_\perp}}a_0\beta_0\xi - \frac{\cos\alpha\sqrt{k_{m3}}}{\sqrt{k_{m2}\cos^2\alpha + k_{m3}\sin^2\alpha}}, \tag{45}$$

$$\cos\beta_2 = A_2 = 1 - \sqrt{\frac{u_1}{k_{m2}u_\perp}}a_0\beta_0(1-\xi) - \frac{\cos\alpha\sqrt{k_{m3}}}{\sqrt{k_{m2}\cos^2\alpha + k_{m3}\sin^2\alpha}}, \tag{46}$$

where σ_0 — static conductivity, Σ — dimensionless electric conductivity. In expression $k_{m\alpha_0}$ depends on angle α_0, which is expressed through angle α using formula (24). And vice versa, in expressions (45) and (46) we need to express angle α through angle α_0 using the same formula (24).

Conductivity from charge carriers with trajectory, which does not intersect the film borders, is determined by distribution function f_1^{ud}, f_1^{v}. Such conductivity will be called bulk conductivity. It is equal to

$$\Sigma_v = \frac{a_0}{2\pi\nu_0 I_0}\int_0^\infty\int_0^\infty \frac{\sqrt{u_x}e^{u-u_\mu}}{(1+e^{u-u_\mu})^2}B_5\,du_\perp du_x. \tag{47}$$

Conductivity from charge carriers with trajectory, which intersects the film borders, is determined by distribution function f_1^{ud}, f_1^{u} and f_1^{d}. Such conductivity will be called surface, it is equal to difference of total conductivity and bulk conductivity

$$\Sigma_s = \Sigma - \Sigma_v. \tag{48}$$

3. Limit cases

3.1. Degenerate electron gas ($\exp(u_\mu) \gg 1$)

This gas corresponds to high concentration, low effective mass and low temperature of gas of free charge carriers (metal, semiconductor with high concentration of admixtures). Fermi–Dirac distribution function has stepped form

$$f_0 = \begin{cases} 0, & u < u_\mu, \\ 1, & u > u_\mu. \end{cases} \tag{49}$$

In this case the expressions (29) and (36) are converted as follows:

$$u_1 = k_m u_\mu, \quad k_m = \frac{1}{3}\left(\frac{1}{k_{m1}} + \frac{1}{k_{m2}} + k_{m1}k_{m2}\right),$$

$$\rho = \sqrt{\frac{u_\perp}{u_\mu}}, \tag{50}$$

$$\Sigma = \frac{3a_0}{2\pi\nu_0\sqrt{k_{m1}}}\times\int_0^\infty \rho\sqrt{1-\rho^2}(B_1+B_2+B_3+B_4+B_5)d\rho, \tag{51}$$

$$\cos\beta_1 = A_1 = 1 - \frac{1}{\rho}\sqrt{\frac{k_m}{k_{m2}}}\times a_0\beta_0\xi - \frac{\cos\alpha\sqrt{k_{m3}}}{\sqrt{k_{m2}\cos^2\alpha + k_{m3}\sin^2\alpha}}, \tag{52}$$

$$\cos\beta_2 = A_2 = 1 - \frac{1}{\rho}\sqrt{\frac{k_m}{k_{m2}}}\times a_0\beta_0(1-\xi) + \frac{\cos\alpha\sqrt{k_{m3}}}{\sqrt{k_{m2}\cos^2\alpha + k_{m3}\sin^2\alpha}}, \tag{53}$$

3.2. Non-degenerate electron gas ($\exp(-u_\mu) \gg 1$)

This case corresponds to low concentration, high effective mass and high temperature of gas of free charge carriers (semiconductor with low concentration of admixtures). Fermi–Dirac Distribution function will take form of classic Maxwell–Boltzmann distribution:

$$f_0 = \exp\{u_\mu - u\}. \tag{54}$$

In this case the expressions (29) and (36) are converted as follows:

$$u_1 = \frac{5}{2}k_m, \tag{55}$$

$$\Sigma = \frac{a_0}{2\pi\nu_0 k_{m1}^{3/2}}\int_0^\infty e^{-u_\perp}(B_1+B_2+B_3+B_4+B_5)du_\perp. \tag{56}$$

3.3. Spherical constant energy surface ($k_{m1} = k_{m2} = 1$)

Obtained expressions (36)–(46) correspond to electric conductivity obtained in paper [17].

$$\Sigma = \frac{a_0}{\nu_0} - B_{1s} - B_{2s} - B_{3s}, \tag{57}$$

$$B_{1s} = \frac{1}{\nu_0}\int_0^{u_0}\int_{-1}^{1}\sqrt{\frac{u_\perp}{u_1}}D(u_\perp)g_1\left(\frac{\nu_0\varphi_1}{a_0\beta_0}\right)d\eta du_\perp, \tag{58}$$

$$B_{2s} = \frac{1}{\nu_0}\int_{u_0}^{\infty}\int_{-1}^{n_0}\sqrt{\frac{u_\perp}{u_1}}D(u_\perp)g_1\left(\frac{\nu_0\varphi_1}{a_0\beta_0}\right)d\eta du_\perp, \tag{59}$$

$$B_{3s} = \frac{1}{\nu_0}\int_{u_0}^{\infty}\int_{\eta_0}^{1}\sqrt{\frac{u_\perp}{u_1}}D(u_\perp)g_2\left(\frac{\nu_0\varphi_2}{a_0\beta_0}\right)d\eta du_\perp, \tag{60}$$

$$g_1(p) = \frac{2 - q_1 - q_2 - (q_1 + q_2 - 2q_1q_2)e^{-p}}{[1 - q_1e^{-p}][1 - q_2e^{-p}]}[1 - e^{-p}], \tag{61}$$

$$g_2(p) = \frac{2 - q_1 - q_2 + (q_1 + q_2 - 2q_1q_2)e^{-p}}{1 - q_1q_2e^{-2p}}[1 - e^{-p}], \tag{62}$$

$$D(u_\perp) = \frac{a_0}{2\pi\nu_0 I_0}\int\limits_0^\infty \frac{\sqrt{u_x}e^{u_x+u_\perp-u_\mu}}{(1+e^{u_x+u_\perp-u_\mu})^2}du_x, \tag{63}$$

$$\varphi_1 = 2\pi - 2\arccos\eta,$$

$$\varphi_2 = \pi - \arccos\eta - \arccos(\eta_0 - \eta + 1), \tag{64}$$

$$u_0 = \frac{a_0^2\beta_0^2 u_1}{4}, \quad \eta_0 = \beta_0\sqrt{\frac{u_\perp}{u_1}} - 1, \quad u_1 = \frac{5}{4}k_m\frac{I_1}{I_0}. \tag{65}$$

3.4. Thick film ($a \gg \lambda$), mirror surfaces of the film ($q_1 = q_2 = 1$)

Exponents $\exp(\nu_0 k_{m0}\varphi_1/\beta_0 a_0)$ and $\exp(\nu_0 k_{m0}\varphi_2/\beta_0 a_0)$ in expressions (36)–(46) quickly attenuate in case of thick film, high frequency or do not contribute in case of mirror border of film. As a result, the electrical conductivity tends to the following expression:

$$\Sigma = \Sigma_v = \frac{a_0}{\nu_0 k_{m1}}, \tag{66}$$

which corresponds to known Drude formula.

4. Analysis of results

Different values k_{m1} and k_{m2} from expression (28) correspond to different materials at fixed orientation of Spherical constant energy ellipsoid relatively to external electric field. Electric field is oriented along X axis. For silicon $k_{m1} = 2.9$ and $k_{m2} = 0.59$, and for germanium: $k_{m1} = 7.2$ and $k_{m2} = 0.37$, if axis of rotation of ellipsoid is along external field [24].

Dependence of electric conductivity Σ on k_{m1} is obvious: upon increase in effective mass along external field the speed of charge carriers will decrease in this direction. This will result in conductivity decreasing both by absolute value and by argument.

Fig. 3 shows dependence of dimensionless total, bulk and surface conductivity on dimensionless effective mass k_{m2} along axis p_y. At large k_{m2} (or large m_2, as k_{m2} directly proportional to m_2) semi-axis of ellipse z_{01} (11) will extend across the film plane at constant energy $\varepsilon_\perp$ and constant value m_3, i.e. trajectory of charge carriers elongates to film surface. this results in decrease in absolute value of bulk and surface electric conductivity, as contribution of surface scattering increases as compared to contribution of the bulk scattering. At low values of k_{m2} at constant values of $\varepsilon_\perp$ and m_3 semi- axis z_{01} length decreases, which results in decrease in intensity of surface scattering. As a result, the electrical conductivity increases in absolute value. Dependence of bulk conductivity on dimensionless

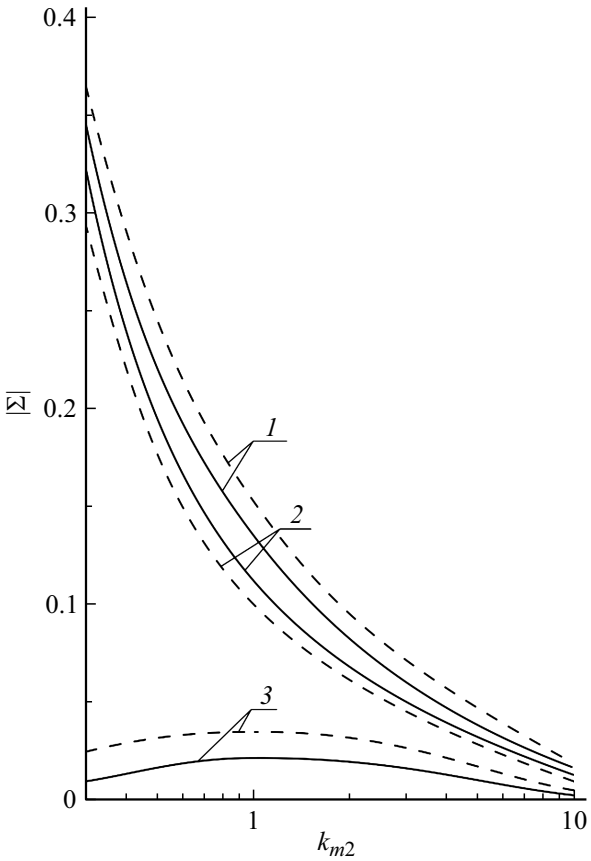

Figure 3. Dependence of absolute value of dimensionless electric conductivity $|\Sigma|$ in degenerate case (solid lines) and in non-degenerate case (dashed lines) on dimensionless effective mass k_{m2} at $k_{m1} = 1$, $a_0 = 0.1$, $\omega_0 = 0.5$, $\beta_0 = 1$, $q_1 = q_2 = 0$. Curves *1–3* correspond to total, surface and bulk conductivities.

effective mass k_{m2} has maximum. This is explained by the fact that if energy $\varepsilon_\perp$ and effective mass m_3 are fixed, then upon $|1 - k_{m2}|$ increasing the length of trajectory increases in transverse cross-section of the film (length of the circumference is less than the perimeter of the ellipse). The increase in the trajectory length leads to increase in the ratio of the scattering frequency in the volume to the scattering frequency on the surface.

Fig. 4 shows dependence of absolute value of dimensioinless electric conductivity on dimensionless effective mass k_{m2} along axis p_y at different values of magnetic induction. With increase in magnetic field induction the ellipse perimeter decreases, as its semi-axes are inversely proportional to the magnetic field induction (11). This results in lower probability of scattering at film borders.

In Fig. 5 the theoretical and experimental dependences of longitudinal relative magnetoresistance are plotted for polycrystalline film of bismuth with orientation (001), which has magnetoresistance similar to magnetoresistance of single-crystal film of bismuth [25]. The film thickness is 29 nm. Dots — experimental data of paper, solid curves — theoretical calculation using formula (34)–(46),

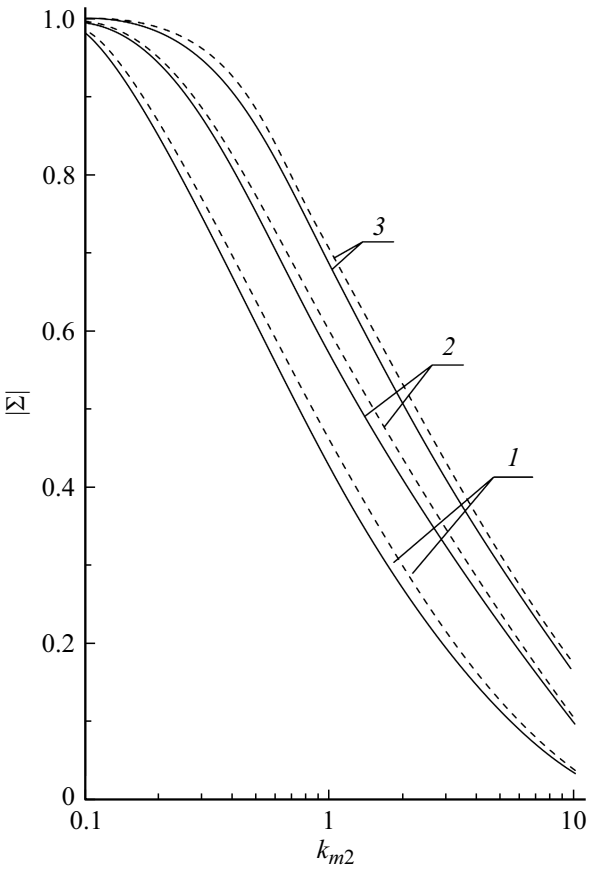

Figure 4. Dependence of absolute value of dimensionless electric conductivity $|\Sigma|$ in degenerate case (solid lines) and in non-degenerate case (dashed lines) on dimensionless effective mass k_{m2} at $k_{m1} = 1$, $a_0 = 0.1$, $\omega_0 = 0.1$, $q_1 = q_2 = 0.2$. Curves *1–3* were obtained at $\beta_0 = 10$, 20, 30 respectively.

(50)–(53). The bismuth film was obtained using molecular-beam epitaxy with rate 1.6 Å/min. The film thickness was measured using field emission microscopy. The magnetoresistance was determined using physical properties measurement system (PPMS).

The constant energy surface for electrons in bismuth is three symmetrically located ellipsoids, which axes of rotation are directed parallel to film plane [26]. Angle between axes of rotation is similar and equal to $2\pi/3$. Conductivity of bismuth film can be determined as follows [27]. Let's $\sigma_{\|}$ and $\sigma_{\perp}$ — electric conductivities determined by one constant energy ellipsoid of bismuth, along and transverse the axis of rotation of this ellipsoid, respectively. Longitudinal mass $m_{\|}$ for $\sigma_{\|}$ or transverse mass $m_{\perp}$ for $\sigma_{\perp}$ is directed along external electric field. If axis of rotation of ellipsoid is parallel to axis p_x, then tensor of conductivity is diagonal:

$$\tilde{\sigma}_0 = \begin{pmatrix} \sigma_{\|} & 0 \\ 0 & \sigma_{\perp} \end{pmatrix}.$$

In case of arbitrary direction of main axis of ellipsoid in plane (p_x, p_y) the expression for tensor of conductivity can be obtained using matrix of rotation around axis p_z:

$$\sigma_{0ij} = M^{v_z}_{ik}(\varphi_0)\tilde{\sigma}_{0kl}M^{v_z}_{lj}(-\varphi_0),$$

where $M^{v_z}_{ik}(\varphi_0)$ — components of matrix of rotation around axis p_z by angle φ_0:

$$M^{v_z}(\varphi_0) = \begin{pmatrix} \cos\varphi_0 & -\sin\varphi_0 \\ \sin\varphi_0 & \cos\varphi_0 \end{pmatrix},$$

where φ_0 — angle between axis of rotation of ellipsoid for $\sigma_{\|}$ and electric field strength.

As result we have the following view of tensor of conductivity:

$$\sigma_0 = \begin{pmatrix} \sigma_{\|}\cos^2\varphi_0 + \sigma_{\perp}\sin^2\varphi_0 & (\sigma_{\|} - \sigma_{\perp})\cos\varphi_0\sin\varphi_0 \\ (\sigma_{\|} - \sigma_{\perp})\cos\varphi_0 sin_0 & \sigma_{\|}\sin^2\varphi_0 + \sigma_{\perp}\cos^2\varphi_0 \end{pmatrix}.$$

σ_0 — electric conductivity of one ellipsoid, for bismuth their number is three, so bismuth conductivity is

$$\sigma_{0\mathrm{Bi}} = \sigma_0(\varphi_0) + \sigma_0\left(\varphi_0 + \frac{2\pi}{3}\right) + \sigma_0\left(\varphi_0 + \frac{4\pi}{3}\right) = \frac{3}{2}(\sigma_{\|} + \sigma_{\perp})\begin{pmatrix} 1 & 0 \\ 0 & 1 \end{pmatrix}.$$

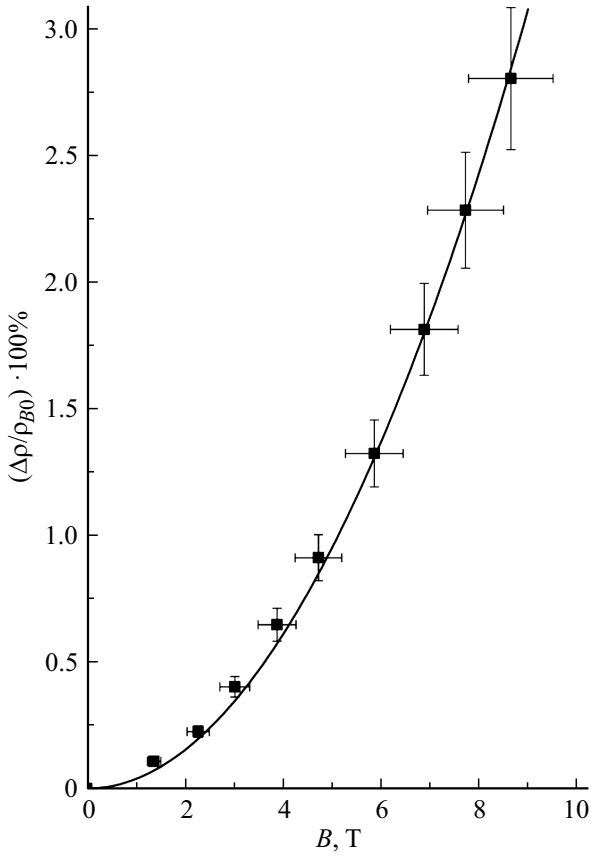

Figure 5. Parallel magnetoresistance of thin film of bismuth vs. magnetic field induction. Dots designate experimental data [26], and solid curve — theoretical calculation.

Thus, electric conductivity does not depend on orientation of ellipsoids, i.e. on angle φ_0. We are interesting only in x-component determined by the electric field along axis X, i.e. component $(\sigma_{0\mathrm{Bi}})_{11}$:

$$(\sigma_{0\mathrm{Bi}})_{11} = \sigma = \frac{3}{2}(\sigma_{\parallel} + \sigma_{\perp}).$$

On graph $\Delta\rho = \rho - \rho_{B0}$, where $\rho = 1/\sigma$ and $\rho_{B0} = 1/\sigma$ $(B = 0)$). For the greatest agreement between the experimental data and the theoretical calculation, the specularity coefficients were taken equal to $q_1 = q_2 = 0.8$.

Conclusion

Analytical expressions are obtained for high frequency electric conductivity of thin film in longitudinal magnetic field considering constant energy surface. Maximum of dependences of absolute value of bulk conductivity on effective mass along film plane is determined. It is shown that with increase in effective mass long film plane the total and surface conductivities decrease in absolute value. There is agreement between theory and experiment for electric conductivity of thin Bi films. Experimental data deviation from theoretical calculation does not exceed 5%.

Conflict of interest

The authors declare that they have no conflict of interest.

References

[1] A.L. Chizh, K.B. Zhuravlev, D.V. Dmitriev, A.I. Toropov, N.A. Valisheva, M.S. Aksenov, A.M. Gilinsky, I.B. Chistokhin. Pis'ma v ZhTF, **45** (14), 52 (2019). (in Russian) DOI: 10.21883/PJTF.2019.14.48026.17764 [A.L. Chizh, K.B. Mikitchuk, K.S. Zhuravlev, D.V. Dmitriev, A.I. Toropov, N.A. Valisheva, M.S. Aksenov, A.M. Gilinsky, I.B. Chistokhin. Tech. Phys. Lett., **45**, 739 (2019). DOI: 10.1134/S1063785019070204]

[2] V.S. Varavin, V.V. Vasilyev, A.A. Guzev, S.A. Dvoretsky, A.P. Kovchavtsev, D.V. Marin, I.V. Sabinina, Yu.G. Sidorov, G.Yu. Sidorov, A.V. Tsarenko, M.V. Yakushev. Semiconductors, **50**, 1626 (2016). DOI: 10.1134/S1063782616120265

[3] L. Wang, M. Yin, A. Khan, S. Muhtadi, F. Asif, E. S. Choi, T. Datta. Phys. Rev. Appl., **9**, 024006 (2018). DOI: 10.1103/PhysRevApplied.9.024006

[4] M.A. Abeed, J.L. Drobitch, S. Bandyopadhyay. Phys. Rev. Appl., **11**, 054069 (2019). DOI: 10.1103/PhysRevApplied.11.054069

[5] A. Kowsar, S.F.U. Farhad, S.N. Sakib. IJRER, **8** (4), 2218 (2018). DOI: 10.20508/ijrer.v11i4.12474.g8350

[6] B. Godefroid, G. Kozyreff. Phys. Rev. Appl., **8** (3), 034024 (2017). DOI: 10.1103/PhysRevApplied.8.034024

[7] S. Bhattacharya, I. Baydoun, M. Lin, S. John. Phys. Rev. Appl., **11** (1), 014005 (2019). DOI: 10.1103/PhysRevApplied.11.014005

[8] V.S. Kalinovskii, E.V. Kontrosh, A.V. Andreeva, V.M. Andreev, V.V. Malyutina-Bronskaya, V.B. Zalesskii, A.M. Lemeshevskaya, V.I. Kuzoro, V.I. Khalimanovich, M.K. Zaitseva. Tech. Phys. Lett., **45**, 850 (2019). DOI: 10.1134/S1063785019080236

[9] A.B. Nikolskaia, M.F. Vildanova, S.S. Kozlov, O.I. Shevaleevskiy. Semiconductors, **52** (1), 88 (2018). DOI: 10.1134/S1063782618010165

[10] L. Moraga, C. Arenas, R. Henriquez, S. Bravo, B. Solis. Phys. B: Condens. Matter., **499**, 17 (2016). DOI: 10.1016/j.physb.2016.07.001

[11] R. Henriquez, S. Oyarzun, M. Flores, M.A. Suarez, L. Moraga, G. Kremer, C.A. Gonzalez-Fuentes, M. Robles, R.C. Munoz. J. Appl. Phys., **108**, 123704 (2010). DOI: 10.1063/1.3525704

[12] R.C. Munoz, M.A. Su'arez, S. Oyarz'un. Phys. Rev. B, **81**, 165408 (2010). DOI: 10.1103/PhysRevB.81.165408

[13] S. Oyarz'un, R. Henríquez, M.A. Su'arez, L. Moraga, G. Kremer, R.C. Munoz. Appl. Surf. Sci., **289**, 167 (2014). DOI: 10.1016/j.apsusc.2013.10.128

[14] A.I. Utkin, A.A. Yushkanov, E.V. Zavitaev. J. Surf. Investigation: X-ray, Synchrotron and Neutron Techniques, **10**, 5 (2016). DOI: 10.1134/S1027451016050153

[15] A.I. Utkin, A.A. Yushkanov. Tech. Phys., **61**, 1457 (2016). DOI: 10.1134/S1063784216100273

[16] I.A. Kuznetsova, O.V. Savenko, A.A. Yushkanov. Tech. Phys., **62**, 1766 (2017). DOI: 10.1134/S1063784217120143

[17] I.A. Kuznetsova, O.V. Savenko, P.A. Kuznetsov. Semiconductors, **54**, 1039 (2020). DOI: 10.1134/S106378262009016X

[18] E.V. Zavitaev, K.E. Kharitonov, A.A. Yushkanov. Tech. Phys., **64**, 593 (2019). DOI: 10.1134/S1063784219050268

[19] I.A. Kuznetsova, D.N. Romanov, A.A. Yushkanov. Russ. Microelectron., **47** (3), 201 (2018). DOI: 10.1134/S1063739718030071

[20] E.H. Sondheimer. Adv. Phys., **50** (6), 499 (2001). DOI: 10.1080/00018730110102187

[21] D.A. Bandurin, I. Torre, R. Krishna Kumar, M. Ben Shalom, A. Tomadin, A. Principi, G.H. Auton, E. Khestanova, K.S. Novoselov, I.V. Grigorieva, L.A. Ponomarenko, A.K. Geim, M. Polini. Science, **351**, 1055 (2016). DOI: 10.1126/science.aad0201

[22] M.J.H. Ku, T.X. Zhou, Q. Li, Yo. J. Shin, J.K. Shi, C. Burch, L.E. Anderson, A.T. Pierce, Yo. Xie, A. Hamo, U. Vool, H. Zhang, F. Casola, T. Taniguchi, K. Watanabe, M.M. Fogler, Ph. Kim, A. Yacoby, R.L. Walsworth. Nature, **583**, 537 (2020). DOI: 10.1038/s41586-020-2507-2

[23] K.S. Denisov, K.A. Baryshnikov, P.S. Alekseev. Phys. Rev. B Lett., **106**, L081113 (2022). DOI: 10.1103/PhysRevB.106.L081113

[24] K.V. Shalimova, Fizika poluprovodnikov: uchebnik (Lan', SPb, 2010) (in Russian)

[25] N. Wang, Y. Qi. Vacuum, **191**, 110360 (2021). DOI: 10.1016/j.vacuum.2021.110360

[26] V.S. Edel'man. UFN, **123** (2), 260 (1977) (in Russian). DOI: 10.3367/UFNr.0123.197710d.0257 [V.S. Édel'man. Sov. Phys. Usp., **20**, 819 (1977). DOI: 10.1070/PU1977v020n10ABEH005467]

[27] I.A. Kuznetsova, O.V. Savenko, D.N. Romanov. Phys. Lett. A, **427**, 127933 (2022). DOI: 10.1016/j.physleta.2022.127933

Translated by I.Mazurov